

## Reaction cross sections for 38, 65, and 97 MeV deuterons on targets from $^9\text{Be}$ to $^{208}\text{Pb}$

A. Auce,<sup>1</sup> R. F. Carlson,<sup>2</sup> A. J. Cox,<sup>2</sup> A. Ingemarsson,<sup>1,3,\*</sup> R. Johansson,<sup>1</sup> P. U. Renberg,<sup>3</sup> O. Sundberg,<sup>3</sup> and G. Tibell<sup>1</sup>

<sup>1</sup>*Department of Radiation Sciences, Box 535, S-75121 Uppsala, Sweden*

<sup>2</sup>*University of Redlands, Redlands, California 92373*

<sup>3</sup>*The Svedberg Laboratory, Box 533, S-75121 Uppsala, Sweden*

(Received 20 February 1996)

Reaction cross sections for deuterons have been measured for  $^9\text{Be}$ ,  $^{12}\text{C}$ ,  $^{16}\text{O}$ ,  $^{28}\text{Si}$ ,  $^{40,48}\text{Ca}$ ,  $^{58,60}\text{Ni}$ ,  $^{112,116,120,124}\text{Sn}$ , and  $^{208}\text{Pb}$  at 37.9, 65.5, and 97.4 MeV. [S0556-2813(96)03806-X]

PACS number(s): 25.45.De, 24.10.Ht

### I. INTRODUCTION

Partial wave analyses of elastic scattering angular distributions result in sets of phase shifts which also uniquely determine the reaction cross sections. In spite of the fact that the analyses of the angular distributions often result in ambiguities for the optical potential, experimental efforts in the past have mainly concentrated on measuring angular distributions for more target nuclei and at new energies, while up to now very few measurements of the complementary reaction cross sections have been performed.

Some years ago we embarked on a program to measure  $^4\text{He}$  reaction cross sections in the energy region 20–50 MeV per nucleon for different nuclei. The original motivation for these measurements was to determine a further constraint on the optical model in the analyses of elastic scattering. It was found [1]; however, that the optical model calculations systematically overestimated the reaction cross sections. We suspected at that time that the discrepancy was due to the fact that oversimplified models were used and that in this case the Woods-Saxon parametrization was inadequate. It turned out [2], however, that the discrepancy increased in analyses using the folding approach, which in detail reproduced the shape of the elastic scattering angular distributions.

These results were very surprising and we therefore decided to perform the same set of measurements for deuterons. It was our hope that results for deuterons would give complementary information to those of  $^4\text{He}$ . The fact that the deuteron is so loosely bound caused us to make a more detailed study of particles emitted in the forward direction. As will be seen later in this report, the results of this experiment suggest that the earlier discrepancy for  $^4\text{He}$  may be

partially of experimental character. We therefore plan to repeat our measurement for  $^4\text{He}$ .

### II. EXPERIMENTAL METHOD

The experimental procedure consisted of a variation of a standard attenuation technique. The method and experimental apparatus, originally designed for measuring proton reaction cross sections, are described in detail in Ref. [3]. This technique was recently applied by the Redlands/Uppsala collaboration in a measurement of reaction cross sections for  $^4\text{He}$  [1], and the reader is referred to these two reports for experimental details.

A well-collimated, momentum analyzed deuteron beam from the Gustaf Werner cyclotron at the Svedberg Laboratory was directed into our apparatus, a schematic diagram of which is given in Fig. 1. The beam energies were determined with a time-of-flight technique. The beam energy spread was approximately 300 keV [full width at half maximum (FWHM)], and the intensity was typically  $2 \times 10^4$  particles per second. Two thin passing scintillators (detectors 1 and 2) and two annular scintillators (detectors 3 and 4) served to identify properly directed deuterons incident on the thin, solid, circular targets, which were approximately 1 cm in diameter. They were mounted on a wheel accommodating 14 targets and an empty space for target-out measurements. Target characteristics are given in Table I. Beyond the target was the stopping detector telescope, comprised of detector 5, a small thin plastic scintillator, and the stopping detector 6, subtending an angle of  $\pm 30^\circ$  as seen from the beam spot on the target.

The electronic logic is shown schematically in Fig. 2. The incident beam intensity  $I_0$  was determined by the signal 12

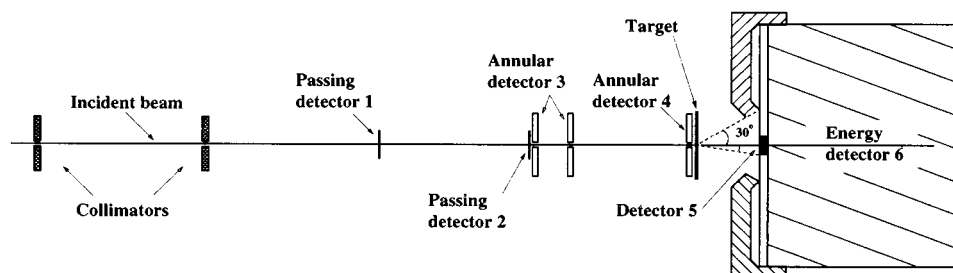


FIG. 1. Schematic diagram of the reaction cross section apparatus.

\*Electronic address: ingo@tsl.uu.se

TABLE I. Target specifications.

Target	Enrichment	Thickness (mg/cm <sup>2</sup> )	Thickness nonuniformity (%)
<sup>9</sup> Be	100%	35.6	1
<sup>12</sup> C	Natural	78.9	0.5
SiO <sub>2</sub>	Natural	62.0	0.1
<sup>28</sup> Si	Natural	77.4	0.1
<sup>40</sup> Ca	Natural	49.0	4
<sup>48</sup> Ca	90.8%	10.9	2
<sup>58</sup> Ni	99.79%	40.5	2
<sup>60</sup> Ni	99.07%	39.5	2
<sup>112</sup> Sn	80.04%	40.8	2
<sup>116</sup> Sn	95.74%	41.5	2
<sup>120</sup> Sn	98.05%	42.5	2
<sup>124</sup> Sn	96.71%	38.5	2
<sup>208</sup> Pb	99.86%	67.4	4

$(\overline{3+4})$ , and the transmitted, nonreacting beam intensity  $I$  by  $12(\overline{3+4})(5+6)$ . A pile-up rejection scheme prohibited both of two consecutive deuterons from producing an  $I_0$  logic signal if they arrived within  $1 \mu\text{s}$  of each other. The corrections necessary to determine the reaction cross section from these raw data are described in the next section.

A series of target-in and target-out measurements, each consisting of either  $10^7$  or  $5 \times 10^6$  incident deuterons, was performed. The uncorrected reaction cross section  $\sigma_{\text{un}}$  was determined from the difference between the term  $(I_0 - I)$  and the corresponding quantity  $(i_0 - i)$  obtained from target-out measurements.

#### A. Corrections to the raw data

The uncorrected reaction cross section  $\sigma_{\text{un}}$  was obtained from

$$\sigma_{\text{un}} = \frac{1}{nx} \left[ \frac{(I_0 - I)}{I_0} - \frac{(i_0 - i)}{i_0} \right], \quad (1)$$

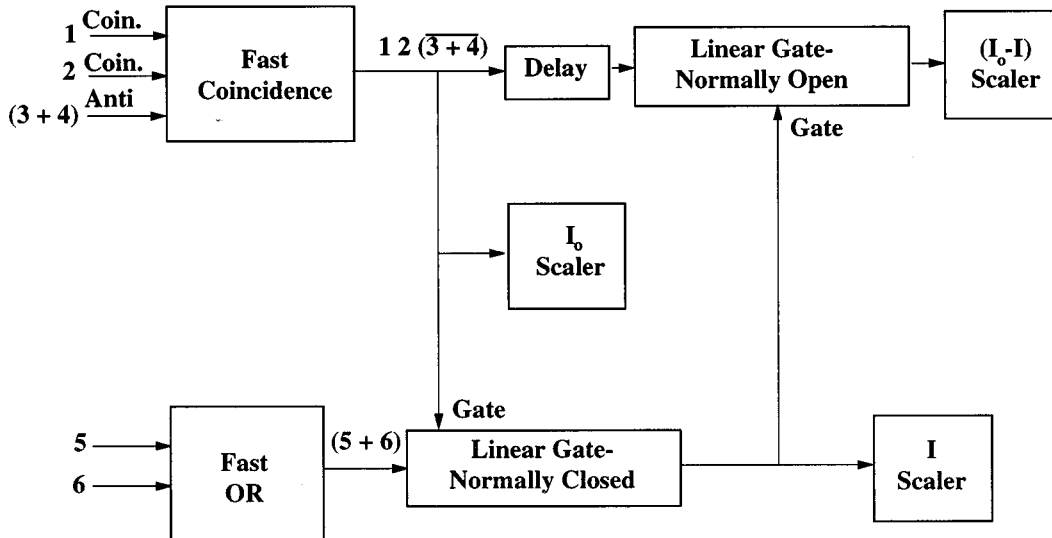


FIG. 2. Schematic diagram of the electronic logic.

where  $n$  is the number of nuclei per unit volume in the target and  $x$  the target thickness.

In the following paragraphs the corrections applied to the raw data are described. They are mostly small and of different signs, so that in the end they almost cancel.

(i) The first correction concerned elastically scattered deuterons which emerged at angles greater than  $30^\circ$  and thus missed detector 6. These nonreaction events were falsely counted as reactions since there was no gate-closing signal from either detector 5 or 6. The experimentally measured  $\sigma_{\text{un}}$  was corrected by subtracting the elastic differential cross section integrated between  $30^\circ$  and  $180^\circ$ . The elastic cross sections were taken from published data [4–23] or calculated from optical potentials in these reports. The correction was negative and less than 9% in all cases.

(ii) The second correction was for nuclear reactions producing charged particles which entered detector 6 ( $\theta < 30^\circ$ ) with energies above the discriminator level for that detector. These were thus falsely counted as elastic events. A correction was applied for these missing reaction events. In most cases the discriminator level for detector 6 was set 8 MeV ( $\Delta E$ ) below the elastic peak at  $E$  MeV for deuterons. Protons produce larger signals in detector 6 (BC400 plastic scintillator) than do deuterons and hence the discriminator level for protons was about 2 MeV lower at the highest energy and about 4 MeV lower at the lowest energy. The contribution for inelastically scattered deuterons, obtained from appropriate published cross sections [4–23], was integrated to give the charged particle reaction correction,

$$2\pi \int_{0^\circ}^{30^\circ} \sin\theta \, d\theta \int_{E-\Delta E}^E \frac{d^2\sigma}{dE d\Omega} dE. \quad (2)$$

Since cross sections for stripping reactions to low-lying levels are generally smaller than those for inelastic scattering, no correction was made for protons producing signals above the discriminator level.

This correction was positive and always less than 3.5% of  $\sigma_{\text{un}}$ .

(iii) Reaction products which triggered detector 5 are, as mentioned above, registered as nonreaction events. In Ref. [1] this correction was measured using a method suggested by an Oak Ridge group [24], based on the assumption that the reaction products are isotropically distributed. Since the loosely bound deuteron has a large probability for breakup and since this process is highly nonisotropic, we decided to study the effect of the finite size of detector 5 by measuring the reaction cross sections with three different sizes of detector 5, covering the angular regions up to  $6.0^\circ$ ,  $7.2^\circ$ , and  $8.9^\circ$ , respectively. It turned out that the effect of the detector size increased with energy, but within the experimental errors the correction was the same for all nuclei at a given energy. At each energy the percentage cross section change for a given nucleus was proportional to the change in solid angle and did not exhibit any dependence on  $\theta$ . Therefore we extrapolated to zero size of detector 5 by applying a correction proportional to the solid angle of detector 5. The correction to the largest size of detector 5 was as large as 2.0%, 4.9%, and 12.4% at the three energies. In our previous measurement for  $\alpha$  particles only the  $8.9^\circ$  size was used. It is because of the importance of this correction that, as mentioned in the Introduction, we have decided to repeat our measurements for  $\alpha$  particles.

TABLE II. Experimental results for the reaction cross sections (mb) for deuterons.

Target	Incident energy (MeV)		
	37.9 $\pm$ 0.2	65.5 $\pm$ 0.5	97.4 $\pm$ 0.3
$^9\text{Be}$	811 $\pm$ 35	633 $\pm$ 23	536 $\pm$ 26
$^{12}\text{C}$	836 $\pm$ 24	678 $\pm$ 15	600 $\pm$ 17
$^{16}\text{O}$	962 $\pm$ 27	811 $\pm$ 19	726 $\pm$ 21
$^{28}\text{Si}$	1199 $\pm$ 35	1083 $\pm$ 21	1023 $\pm$ 25
$^{40}\text{Ca}$	1439 $\pm$ 43	1338 $\pm$ 28	1260 $\pm$ 30
$^{48}\text{Ca}$	1653 $\pm$ 75	1564 $\pm$ 71	1424 $\pm$ 47
$^{58}\text{Ni}$	1625 $\pm$ 51	1571 $\pm$ 33	1524 $\pm$ 45
$^{60}\text{Ni}$	1698 $\pm$ 49	1619 $\pm$ 34	1588 $\pm$ 40
$^{112}\text{Sn}$	2130 $\pm$ 76	2156 $\pm$ 47	2212 $\pm$ 59
$^{116}\text{Sn}$	2174 $\pm$ 69	2257 $\pm$ 49	2254 $\pm$ 53
$^{120}\text{Sn}$	2240 $\pm$ 69	2346 $\pm$ 51	2351 $\pm$ 55
$^{124}\text{Sn}$	2282 $\pm$ 90	2332 $\pm$ 57	2343 $\pm$ 59
$^{208}\text{Pb}$	2844 $\pm$ 142	3049 $\pm$ 71	3250 $\pm$ 82

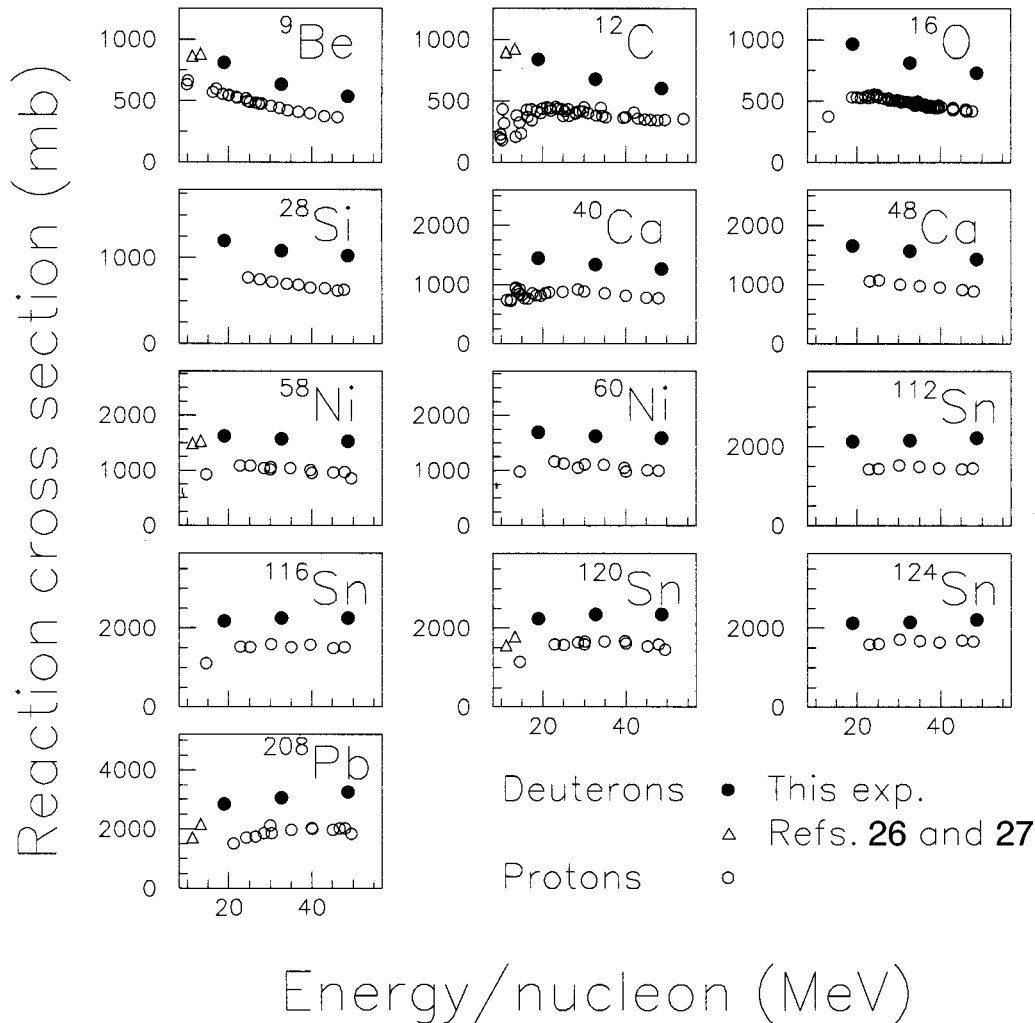


FIG. 3. Experimental values for deuteron and proton reaction cross sections.

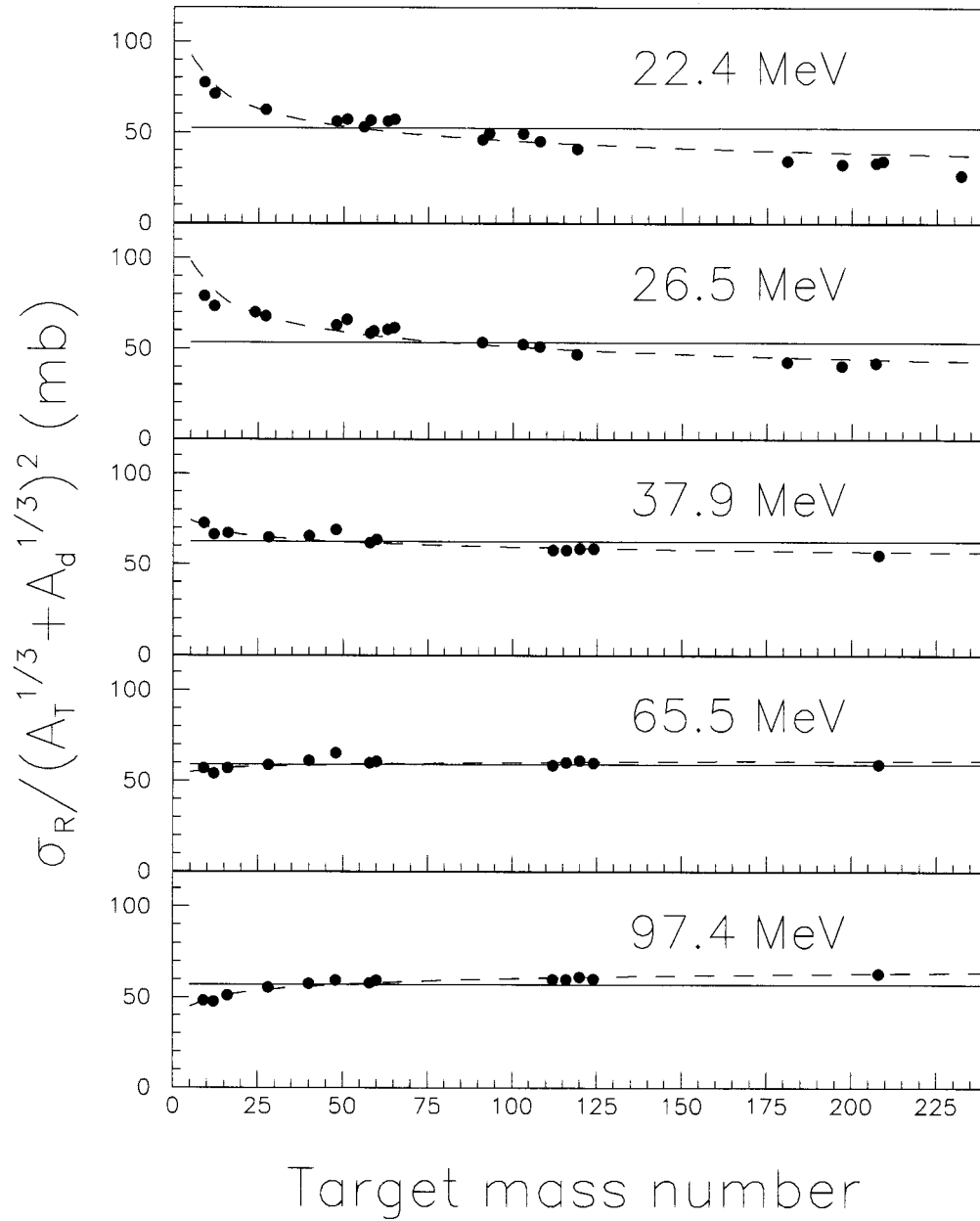


FIG. 4. Experimental values for deuteron reaction cross section divided by  $(A_T^{1/3} + A_d^{1/3})^2$  plotted versus the atomic number  $A_T$ . The dashed and solid curves show the parametrizations with Eq. (3) and Eq. (4), respectively.

(iv) Some deuterons were elastically scattered outside detector 5 but into detector 6 and then lost energy through nuclear reactions in the detector material, thus producing false reaction events. The presence of detector 5 significantly reduced the number of such events. In order to estimate this correction a separate experiment was performed to measure the reaction rate for deuterons in detector 6, using the technique reported in Ref. [25]. The number of deuterons entering detector 5 was counted during the experiment for the purpose of this correction. The correction was negative and less than 1.5% for all nuclei.

(v) Corrections due to finite target thickness and finite beam size were estimated to be negligible.

### III. EXPERIMENTAL RESULTS

The reaction cross sections obtained at the three energies are presented in Table II. The quoted errors are statistical. The results from this experiment are shown in Fig. 3 by the filled circles. The open triangles show the results obtained by Wilkins and Igo at 22.4 MeV [26] and by Mayo *et al.* at 26.5 MeV [27]. It should be noticed that these two measurements were performed with natural targets. Proton reaction cross sections are shown by open circles at the same energy per nucleon. Data were taken from the compilation by one of the present authors [28]. As seen our data are in reasonable agreement with those obtained at 22.4 and 26.5 MeV. As expected, the reaction cross sections are generally larger for

TABLE III. Best fit parameter values obtained with the reaction cross sections parametrized according to Eqs. (3) and (4) for deuterons.

$E$ (MeV)	Eq. (3)		Eq. (4)		
	$r_0$ (fm)	$\chi^2$	$r_T$ (fm)	$r_p$ (fm)	$\chi^2$
22.4 [26]	1.291	596	0.680	3.118	66.2
26.5 [27]	1.302	614	0.773	3.119	76.2
37.9	1.411	58.2	1.213	1.978	11.2
65.5	1.369	35.5	1.445	1.150	19.7
97.4	1.347	120.8	1.580	0.671	8.6

deuterons than for protons. The difference, however, varies from nucleus to nucleus with respect to amplitude as well as energy dependence. For protons as well as for deuterons

there is a general trend that the reaction cross sections decrease with energy for light nuclei and increase for heavy nuclei.

#### IV. PARAMETRIZATION OF THE EXPERIMENTAL RESULTS

We found in Ref. [1] that the reaction cross sections for  $^4\text{He}$  were surprisingly well described by the two parametrizations

$$\sigma_R = \pi r_0^2 (A_T^{1/3} + A_p^{1/3})^2, \quad (3)$$

and

$$\sigma_R = \pi (r_T A_T^{1/3} + r_p A_p^{1/3})^2, \quad (4)$$

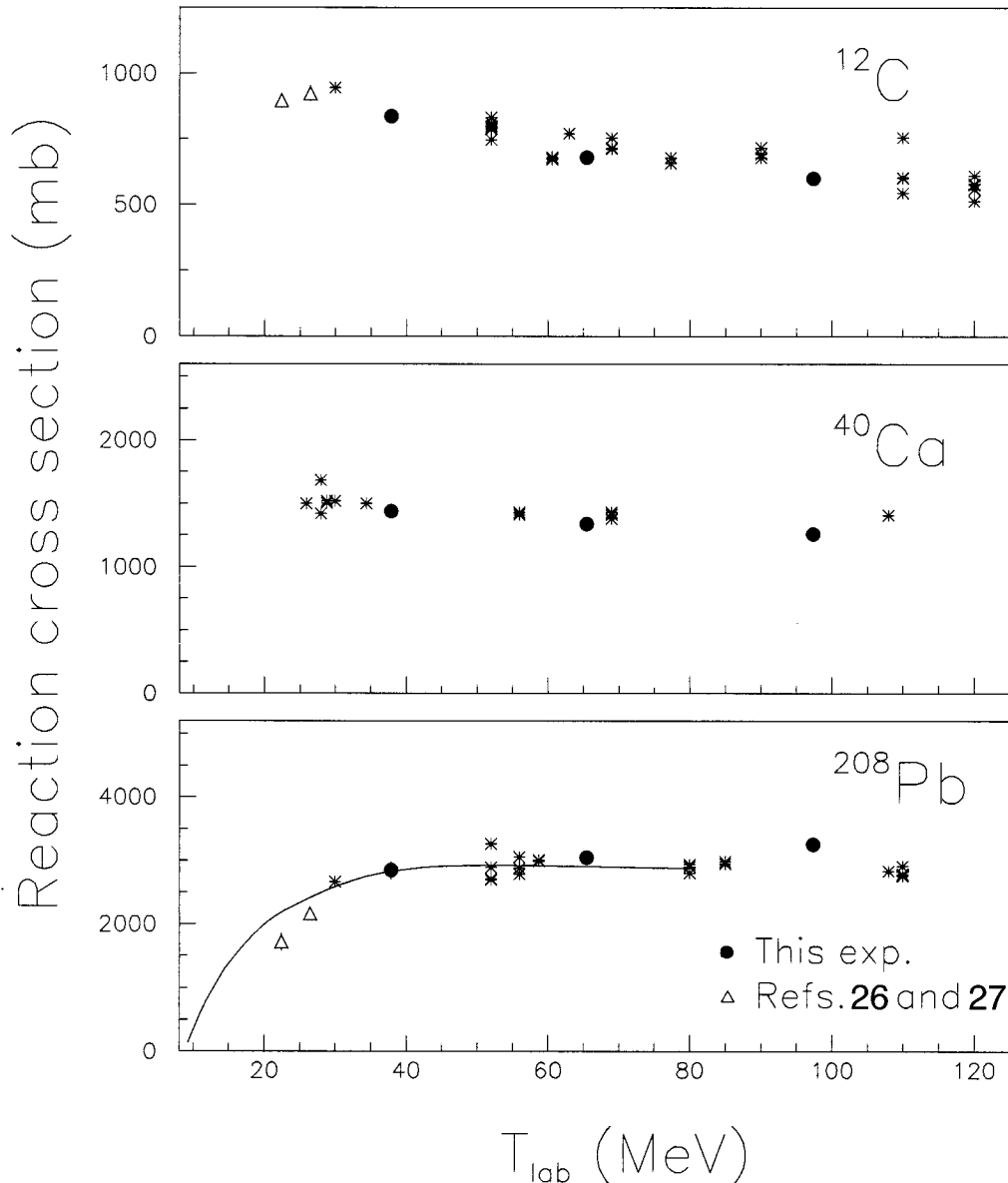


FIG. 5. Experimental values for deuteron reaction cross section compared with predictions from optical model calculations (asterisks) for  $^{12}\text{C}$ ,  $^{40}\text{Ca}$ , and  $^{208}\text{Pb}$ . The solid curve for  $^{208}\text{Pb}$  shows the results obtained by Wang *et al.* [29] using a dispersive optical model potential.

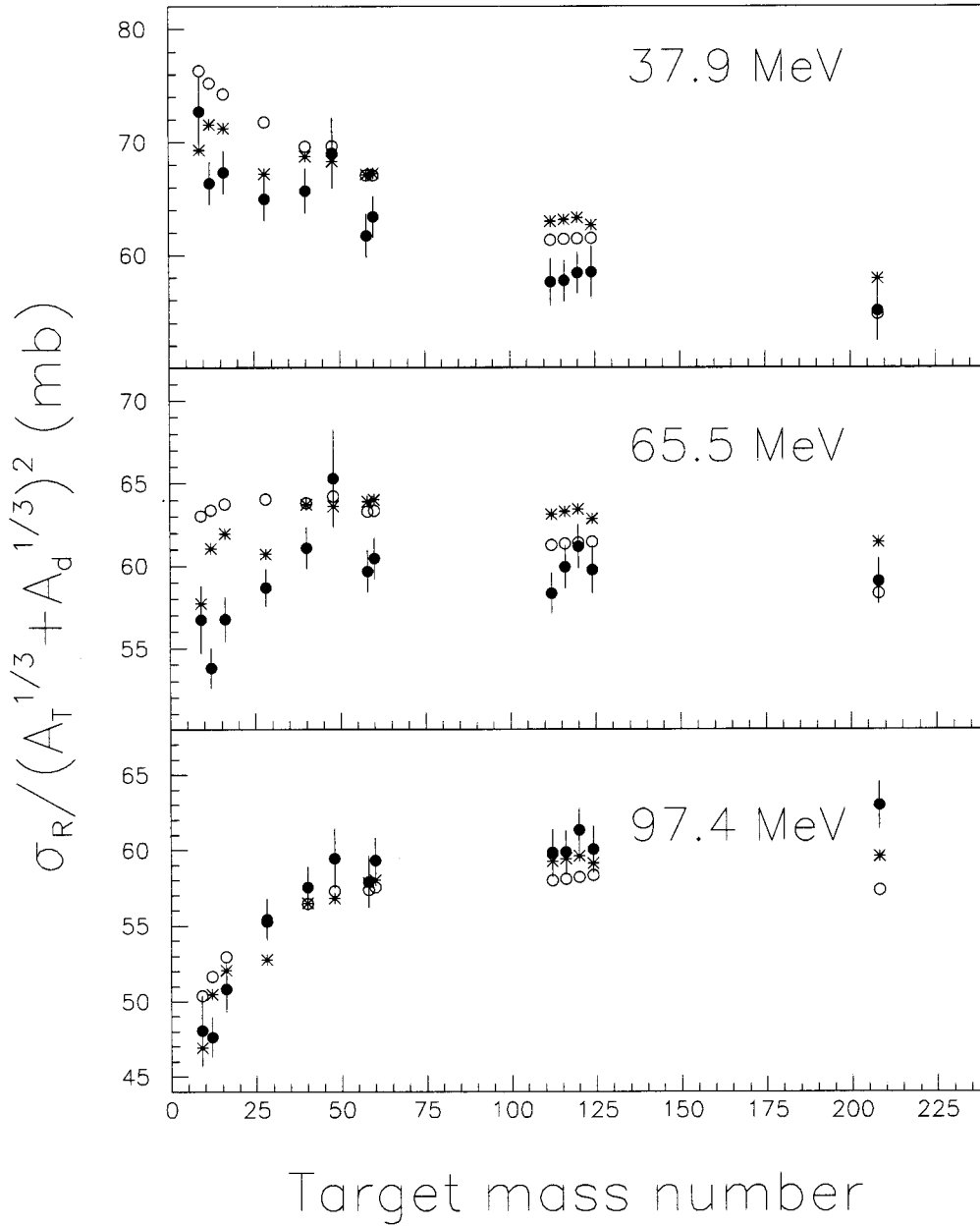


FIG. 6. Experimental values for deuteron reaction cross sections divided by  $(A_T^{1/3} + A_d^{1/3})^2$  compared with predictions by the global potentials in Refs. [14] (\*) and [22] (○).

where  $A_T$  and  $A_p$  are the mass numbers of the target and projectile, respectively. As mentioned in the Introduction, there may be systematic errors in our previous measurement for  $^4\text{He}$ . We believe, however, that these errors are principally related to the energy dependence and only to a small extent to the dependence on atomic number.

Figure 4 shows the results for the reaction cross sections divided by  $(A_T^{1/3} + A_p^{1/3})^2$  for our results as well as for those from Refs. [26] and [27]. The solid lines show the best fits obtained with Eq. (3) and the dashed curves those obtained with Eq. (4). The resulting best fit values are given in Table III. Figure 4 shows that the reaction cross sections divided by  $(A_T^{1/3} + A_p^{1/3})^2$  decrease with increasing atomic number at low energies and increase at high energies. Exactly the same observation was made for  $^4\text{He}$  in Ref. [1] and the transition

from a decrease to an increase with increasing atomic number appears at about the same energy per nucleon.

## V. OPTICAL MODEL CALCULATIONS

Most reports on the elastic scattering of deuterons [4–23] contain one or more optical potentials which reproduce the angular distributions. With some of these potentials we calculated the reaction cross sections for  $^{12}\text{C}$ ,  $^{40}\text{Ca}$ , and  $^{208}\text{Pb}$ . The results obtained are shown in Fig. 5 (asterisks) together with our experimental values (solid circles) as well as those from Refs. [26] and [27] (open triangles). In some cases several potentials have been obtained from the same data set and it is seen that the difference in the calculated reaction cross sections using these potentials is considerably

larger than the experimental errors. The agreement between the experimental and theoretical values is satisfactory, and it is evident that the reaction cross section gives a very important constraint on optical model calculations. In the case of  $^{208}\text{Pb}$ , the solid curve shows the result obtained by Wang *et al.* [29] using a dispersive optical model potential. As seen, our values obtained at the two lower energies are in excellent agreement with their prediction.

Daehnick *et al.* [14] and Bojowald *et al.* [22] have derived global potentials for the elastic scattering of deuterons. Figure 6 shows our experimental values divided by  $(A_T^{1/3} + A_d^{1/3})^2$  (solid circles) together with the results obtained with the global potential by Bojowald *et al.* [22] ( $\circ$ ) and those obtained with the potential by Daehnick *et al.* [14] (\*). With respect to the large variation in the values for the reaction cross section for potentials reproducing the same angular distributions, the results obtained with the global potentials are surprisingly good.

## VI. CONCLUSIONS

We have reported results for reaction cross sections for deuterons at three energies above 30 MeV, a region which

had not been studied earlier. We have observed that the reaction cross section decreases with increasing energy for light nuclei whereas it increases for heavy nuclei. The reaction cross sections tend to be proportional to  $(A_T^{1/3} + A_p^{1/3})^2$  around 40–60 MeV. At lower energies and for light nuclei the reaction cross sections are underestimated by such a proportionality; at higher energies the situation is the opposite. The results obtained are reasonably well reproduced by optical model calculations. Also, the global potentials derived by Daehnick *et al.* [14] and by Bojowald *et al.* [22] reproduce the experimental values well. We believe that the results we have reported have considerably improved the possibilities to derive more reliable potentials for the elastic scattering of deuterons.

## ACKNOWLEDGMENTS

We wish to thank Robert G. Egan for his help in calculating some of the corrections used in the data analysis and Robert Peterson for skilful technical assistance. R.F. Carlson wishes to acknowledge support from a William and Flora Hewlett Foundation grant from the Research Corporation.

- 
- [1] A. Auce, R. F. Carlson, A. J. Cox, A. Ingemarsson, R. Johansson, P. U. Renberg, O. Sundberg, G. Tibell, and R. Zorro, *Phys. Rev. C* **50**, 871 (1994).
- [2] H. Abele, U. Atzrott, A. Auce, C. Hillenmayer, A. Ingemarsson, and G. Staudt, *Phys. Rev. C* **50**, R10 (1994).
- [3] R. F. Carlson, W. F. McGill, T. H. Short, J. M. Cameron, J. R. Richardson, W. T. H. van Oers, J. W. Verba, P. Doherty, and D. J. Margaziotis, *Nucl. Instrum. Methods* **123**, 509 (1975).
- [4] F. Hinterberger, G. Mairle, U. Schmidt-Rohr, G. J. Wagner, and P. Turek, *Nucl. Phys.* **A115**, 570 (1968).
- [5] G. Duhamel, L. Marcus, H. Langevin-Joliot, J. P. Didelez, P. Narboni, and C. Stephen, *Nucl. Phys.* **A174**, 485 (1971).
- [6] G. H. Harrison, University of Maryland progress report, 1972, p. 32.
- [7] G. H. Harrison and P. G. Roos, Report No. ORO-3491-20, 1972, p. 32.
- [8] G. F. Burdzik, C. C. Chang, K. Kwiatkowski, F. E. Bertrand, D. C. Kocher, and E. Newman, University of Maryland progress report 1974, p. 24.
- [9] M. D. Cooper, W. F. Hornyak, and P. G. Roos, *Nucl. Phys.* **A218**, 249 (1974).
- [10] G. Duhamel, H. Langevin-Joliot, J. P. Didelez, E. Gerlic, and J. Van de Wiele, *Nucl. Phys.* **A231**, 349 (1974).
- [11] O. Aspelund, G. Hrehuss, A. Kiss, K. T. Knopfle, C. Mayer-Bricke, M. Rogge, U. Schwinn, Z. Seres, and P. Turek, *Nucl. Phys.* **A253**, 263 (1975).
- [12] C. C. Chang, F. E. Bertrand, and D. C. Kocher, *Phys. Rev. Lett.* **34**, 221 (1975).
- [13] G. Perrin, Nguyen Van Sen, J. Arvieux, R. Darves-Blanc, J. L. Durand, A. Fiore, J. C. Gondrand, F. Merchez, and C. Perrin, *Nucl. Phys.* **A282**, 221 (1977).
- [14] W. W. Daehnick, J. D. Childs, and Z. Vrcelj, *Phys. Rev. C* **21**, 2253 (1980).
- [15] K. Hatanaka, K. Imai, S. Kobayashi, T. Matsusue, M. Nakamura, K. Nisimura, T. Noro, H. Sakamoto, H. Shimizu, and J. Shirai, *Nucl. Phys.* **A340**, 93 (1980).
- [16] A. Willis, M. Morlet, N. Marty, R. Frascaria, C. Djalali, V. Comparat, and P. Kitching, *Nucl. Phys.* **A344**, 137 (1980).
- [17] H. Amakawa and T. Tamura, *Phys. Lett.* **103B**, 393 (1981).
- [18] J. R. Shepard, E. Rost, and D. Murdock, *Phys. Rev. Lett.* **49**, 14 (1982).
- [19] S. N. Mukherjee, L. N. Pandey, D. K. Srivastava, and N. K. Ganguly, *Phys. Rev. C* **29**, 1095 (1984).
- [20] S. M. Banks, B. M. Spicer, G. G. Shute, V. C. Officer, G. J. Wagner, W. E. Dollhopf, Li Qingli, C. W. Glover, D. W. Devins, and D. L. Friesel, *Nucl. Phys.* **A437**, 381 (1985).
- [21] H. Clement, M. Ermer, P. Grabmayr, and G. J. Wagner, in *Proceedings of the International N.P. Conference*, Harrogate, U.K., 1986, p. 11.
- [22] J. Bojowald, H. Machner, H. Nann, W. Oelert, M. Rogge, and P. Turek, *Phys. Rev. C* **38**, 1153 (1988).
- [23] A. C. Betker, C. A. Gagliardi, D. R. Semon, R. E. Tribble, H. M. Xu, and A. F. Zaruba, *Phys. Rev. C* **48**, 2085 (1993).
- [24] J. J. H. Menet, E. E. Gross, J. J. Malanify, and A. Zucker, *Phys. Rev. C* **4**, 1114 (1971).
- [25] For example, see A. M. Sourkes, M. S. de Jong, C. A. Gouling, W. T. H. van Oers, E. A. Ginkel, R. F. Carlson, A. J. Cox, and D. J. Margaziotis, *Nucl. Instrum. Methods* **143**, 589 (1977).
- [26] B. Wilkins and G. Igo, *Phys. Lett.* **3**, 48 (1962).
- [27] S. Mayo, W. Schimmerling, M. J. Sametband, and R.M. Eisberg, *Nucl. Phys.* **62**, 393 (1965).
- [28] R. F. Carlson, *At. Data Nucl. Data Tables* (to be published).
- [29] Y. Wang, C. C. Foster, E. J. Stephenson, Li Yuan, and J. Rapaport, *Phys. Rev. C* **45**, 2891 (1992).